

PROCEEDINGS OF SPIE

SPIEDigitalLibrary.org/conference-proceedings-of-spie

Augmented reality-assisted biopsy of soft tissue lesions

Bettati, Patric, Chalian, Majid, Huang, James, Dormer, James, Shahedi, Maysam, et al.

Patric Bettati, Majid Chalian, James Huang, James D. Dormer, Maysam Shahedi, Baowei Fei, "Augmented reality-assisted biopsy of soft tissue lesions," Proc. SPIE 11315, Medical Imaging 2020: Image-Guided Procedures, Robotic Interventions, and Modeling, 113150W (16 March 2020); doi: 10.1117/12.2549381

SPIE.

Event: SPIE Medical Imaging, 2020, Houston, Texas, United States

Augmented Reality-Assisted Biopsy of Soft Tissue Lesions

Patric Bettati¹, Majid Chalian², James Huang¹, James D. Dormer¹, Maysam Shahedi¹, Baowei Fei^{1,3*}

¹*Department of Bioengineering, University of Texas at Dallas, Richardson, TX*

²*Department of Radiology, Musculoskeletal Imaging and Intervention,
University of Texas Southwestern Medical Center, Dallas, TX*

³*Department of Radiology and Advanced Imaging Research Center,
University of Texas Southwestern Medical Center, Dallas, TX*

*E-mail: bfei@utdallas.edu, Website: <https://fei-lab.org>

ABSTRACT

Guided biopsy of soft tissue lesions can be challenging in the presence of sensitive organs or when the lesion itself is small. Computed tomography (CT) is the most frequently used modality to target soft tissue lesions. In order to aid physicians, small field of view (FOV) low dose non-contrast CT volumes are acquired prior to intervention while the patient is on the procedure table to localize the lesion and plan the best approach. However, patient motion between the end of the scan and the start of the biopsy procedure can make it difficult for a physician to translate the lesion location from the CT onto the patient body, especially for a deep-seated lesion. In addition, the needle should be managed well in three-dimensional trajectories in order to reach the lesion and avoid vital structures. This is especially challenging for less experienced interventionists. These usually result in multiple additional image acquisitions during the course of procedure to ensure accurate needle placement, especially when multiple core biopsies are required. In this work, we present an augmented reality (AR)-guided biopsy system and procedure for soft tissue and lung lesions and quantify the results using a phantom study. We found an average error of 0.75 cm from the center of the lesion when AR guidance was used, compared to an error of 1.52 cm from the center of the lesion during unguided biopsy for soft tissue lesions while upon testing the system on lung lesions, an average error of 0.62 cm from the center of the tumor while using AR guidance versus a 1.12 cm error while relying on unguided biopsies. The AR-guided system is able to improve the accuracy and could be useful in the clinical application.

Keywords: Augmented Reality, Image-guided Biopsy, Biopsy Phantom, Lung Lesion, Soft Tissue, Computed Tomography

1. INTRODUCTION

Biopsies are essential components in diagnosing cancer patients. A biopsy is a method of removing a section of a lesion with the intent of running tests to find out whether the lesion is malignant or not, generally using a thick needle. Since biopsies require puncturing into the body, it can get very difficult to locate the lesion and retract a sample for study. Moreover, some lesions can be very similar to the surrounding tissue, making it impossible to tell if the sample of tissue taken is, in fact, the lesion or simply the surrounding tissue. This can lead to false-negative diagnoses, resulting in the patient not receiving prompt treatment. As such, various methods are used to increase biopsy accuracy, namely using various imaging techniques in conjunction with performing a biopsy.

Different modalities have been used image-guided biopsy, including ultrasound (US), computed tomography (CT), magnetic resonance imaging (MRI), and electromagnetic tracking to improve accuracy and decrease complication rates¹⁻⁷. Among these, CT is being used more frequently due to its availability, reduced operator dependability, powerful depth visualization, and reasonable cost. Traditionally, CT-guided needle biopsies are based on CT volumes obtained prior to intervention⁸, with potentially multiple image acquisition sessions needed per biopsy to localize the lesion in addition to multiple intra-procedural imaging to guide the pathway of the biopsy needle in relation to the targeted lesion⁹. However, these volumes can be difficult for an interventionist to mentally register to a patient after imaging when it comes time to perform the biopsy^{8, 10}. This could result in the physician missing the lesion

during biopsy, especially when multiple small lesions might be present. In addition, this process exposes such patients to increased risk of ionizing radiation especially in this patient population when multiple screening CT imageries are acquired for staging and to monitor disease progression.

To increase the accuracy of soft tissue biopsies, decrease turn-around-time (TOT) of the procedure, and to decrease exposure to unnecessary radiation dose, we propose an augmented reality workflow and present a procedure to superimpose the tumor visually onto the patient using a set of augmented reality glasses and the initial CT images. In order to validate our system, we created a series of phantoms to simulate difficult biopsy conditions, where a soft tissue lesion is located in a difficult to reach location. This work presents how an augmented reality-guided system can be used to increase the biopsy accuracy and reduce the number of scans needed during the procedure. This system requires no additional tracking equipment other than the AR headset, facilitating clinical translation. We also introduce the use of Unity and the HoloLens to create and visualize certain paths of entry to the lesion.

2. METHODS

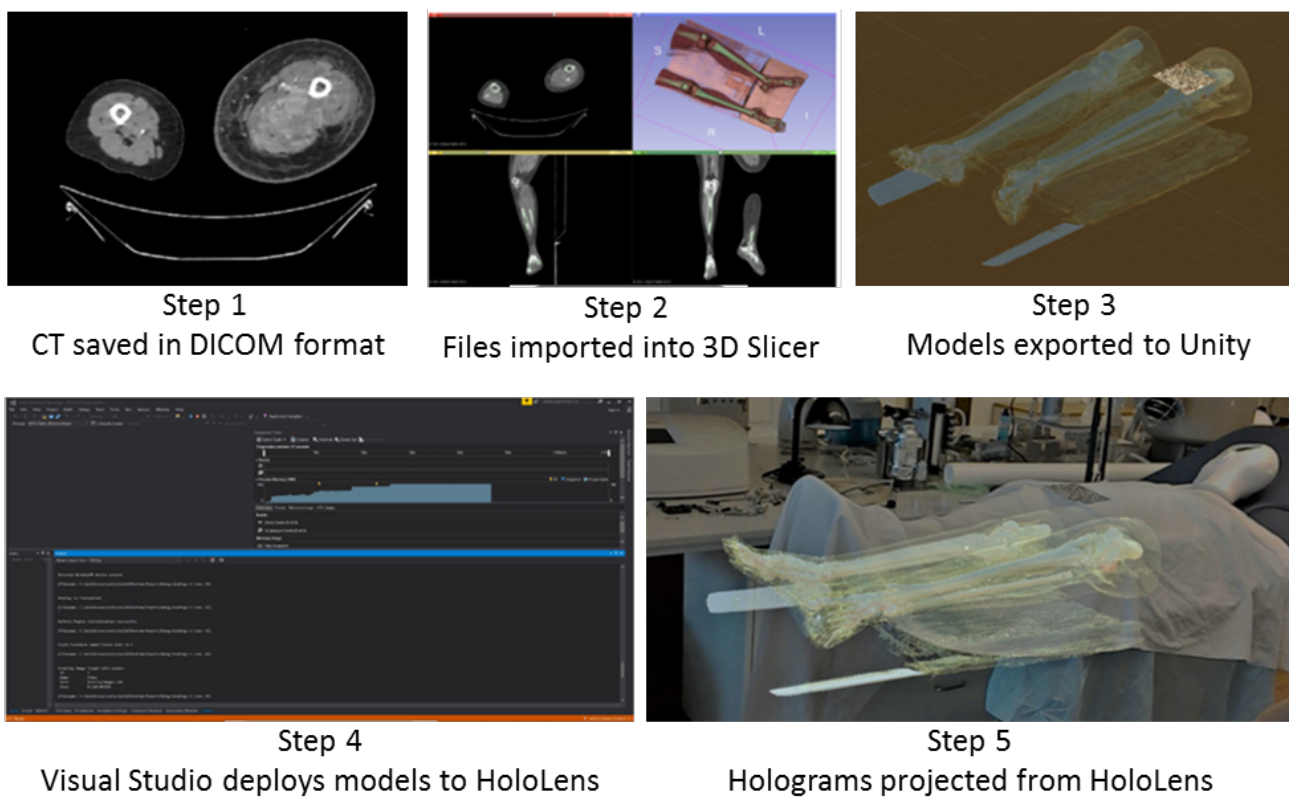


Figure 1: A flow chart depicting an overview of the system. First, a patient CT is acquired, and the data is saved in DICOM format. Next, the DICOM files are imported into 3D Slicer for model generation. These models are then exported separately into Unity to create a complete hologram, which is deployed to the HoloLens using Visual Studio 2017. Finally, the holograms are visualized using the HoloLens.

Model Preparation

The workflow for model generation is shown in Figure 1. Pre-procedure planning CT images of a patient are acquired and saved in DICOM format. Next, the lesion is manually segmented by a fellowship-trained musculoskeletal

radiologist. Additional segmentation volumes of the bones and skin are extracted using 3D Slicer and thresholding and region of interest (ROI) restrictions. The region containing the 3D model is cropped and the resolution reduced in order to improve the visual display through the HoloLens. The models of the bones, skin, and lesion are then exported separately into Unity. From Unity, the models are loaded in a set of Microsoft HoloLens¹¹, with the models being aligned to fiducial markers placed on the leg using Vuforia¹².

Overlays of the segmented skin on top of the patient allow the interventionist to visually check the accuracy of the model-to-patient registration. Once confirmed, the physician can align the biopsy needle to the lesion, avoiding any bones or other regions due to the addition segmentation overlay provided by the HoloLens without requiring additional imaging modalities for needle tracking (Figure 2).

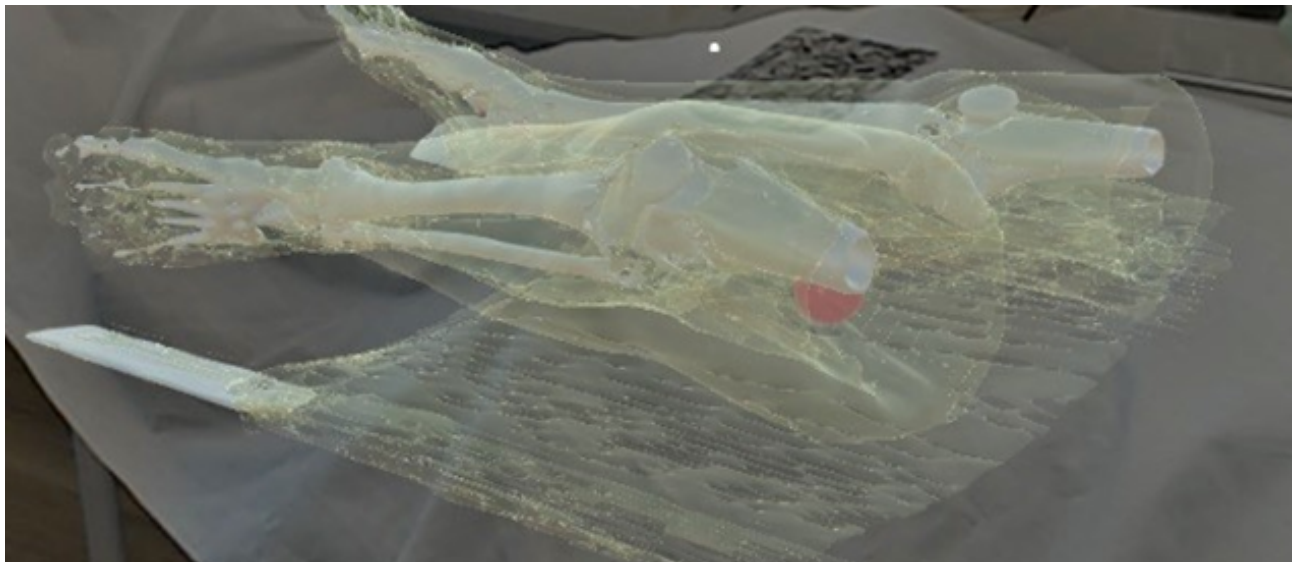


Figure 2: Sample picture taken from HoloLens depicting what a surgeon may see including skin, bones and tumor (red).

Phantom Study

We employed a phantom approach to demonstrate proof of concept under complex needle-path restrictions. To do this, a series of phantom models were developed to approximate the region of biopsy in order to validate the accuracy of our method. The phantoms are created by using a 3% agar solution and pouring the solution into a 12.75 cm x 12.5 cm mold. The lesion was simulated using a 1.5 cm spherical mold, filled with a 4% agar solution and stained with red tissue dye. This is then encased in another spherical 4% agar phantom dyed yellow with a diameter of 2.5 cm, in order to best judge the accuracy of the system. Finally, over the top of the phantom, a layer of 1 cm thick 3% agar solution with blue tissue dye was poured to simulate the region of avoidance, with various holes cut into the layer to simulate the required paths through which the biopsy must be performed.

The phantom is precisely measured, and a 3D model of the phantom is created in Unity (Figure 3A). A marker is added to the hologram to align the model to the physical phantom. The phantom is then covered, and biopsies are performed using standard biopsy needles (Figure 3B)¹³.

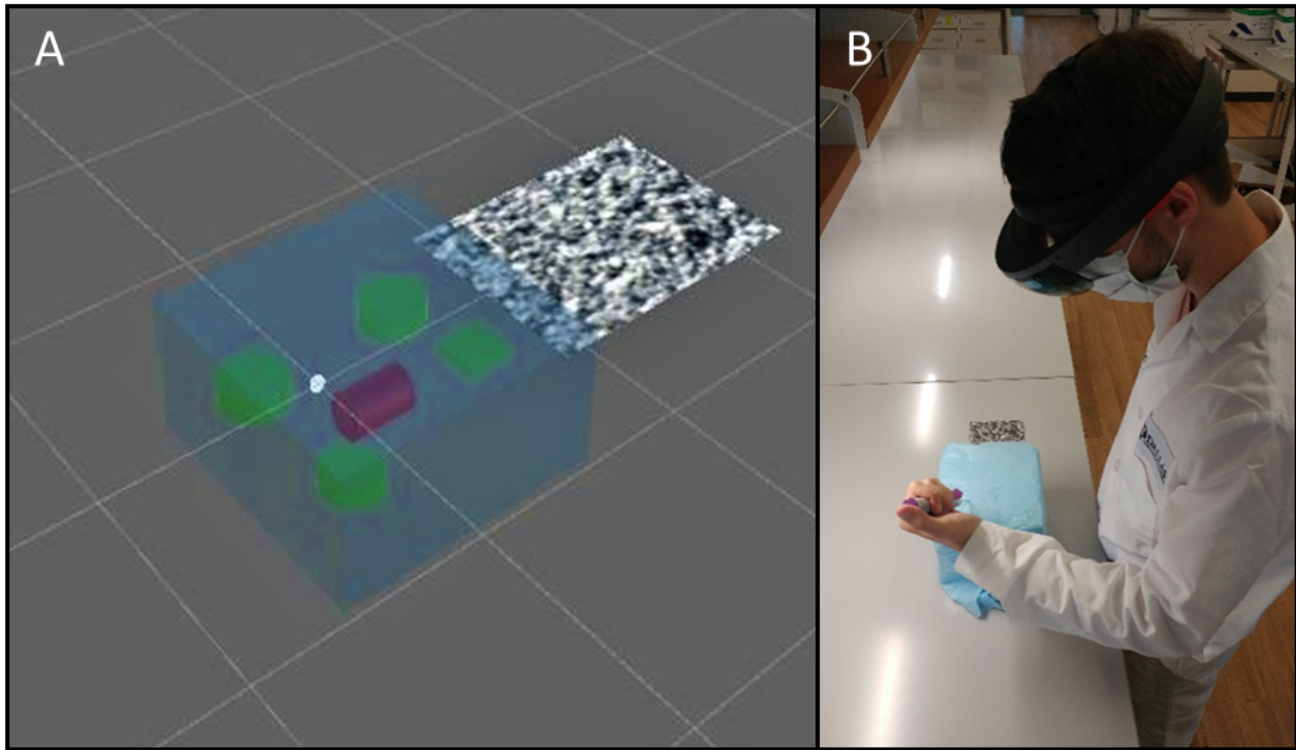


Figure 3. **A:** A Unity example model of one of the phantoms created from synthetic data. **B:** An example of the biopsy procedure, with the phantom covered with an opaque material to simulate skin.

Evaluation

To validate our results on each phantom, we used Euclidean distance; as the tumor is simulated by a sphere in the phantom, the center of the sphere was assigned as the origin of the system. Upon biopsy needle entry, the phantom was cut open along the needle path, allowing a cross-sectional view of the biopsy result in the phantom. The distance from the center of the tumor to the point closest on the final 2.5 cm of the needle path was measured.

Another method of determining accuracy was to measure not from the center of the tumor, but from the edge of the tumor (Figure 4). This means if the tumor was included in the core sample, we set the error value to 0 cm from the edge of the tumor. Upon missing the tumor, we measure from where a core sample was obtained to the closest edge of the tumor. This is a differing method of determining accuracy, which was included in order to display multiple accuracy determinations. We then find the average and standard deviations for each category (AR assisted from center, AR assisted from edge, CT-only from center, CT-only from edge) using the Euclidean distance.

Method Extension to Lung Lesions

The proposed workflow was also evaluated on a more complex biopsy location: lung lesions. The system of model generation and tumor validation remained largely the same, with minor differences specifically in model generation and phantom construction.

We utilized previously acquired images of patients with lung lesions to generate the required models. The main difference between the lung and soft tissue models were that generally the soft tissue lesion models usually contained one bone as a region of avoidance whereas the lung lesion models required multiple ribs as areas of avoidance in addition to the sternum and the heart, depending on the location of the lesion.

To generate these more complex 3D models of the lung lesion area, we segmented out the bones using thresholding of the Hounsfield units between 135 and 1800. However, segmentation of the heart and lesion required manual segmentation through 3D Slicer. We then loaded the model into Unity and deployed the model to the HoloLens using the same method detailed above.



Figure 4: An example of error calculation on a missed biopsy attempt. Needle path is highlighted by a red circle.

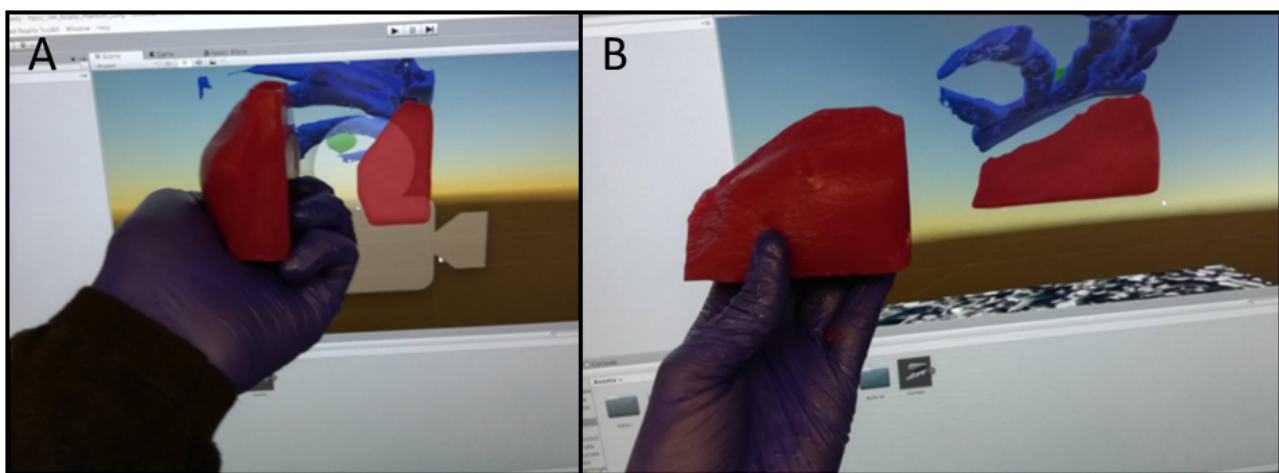


Figure 5. A: Side by side depiction of the similarities between phantom parts and hologram model of the heart, as seen in the narrow field-of-view. **B:** The same model viewed from a different direction.

Creation of the lung lesion phantoms for method evaluation required precise and accurate dimensions on the bone, lesion and heart regions to allow for seamless superimposition between hologram and phantom to allow for greatest biopsy accuracy (Figure 5). To this end, we took precise measurements of each aspect of the model and manually shaped each aspect of the phantom to match the dimensions of the hologram perfectly. An example of a lung lesion phantom is shown in Figure 6. We then proceeded to obtain biopsy samples using the standard aforementioned method.

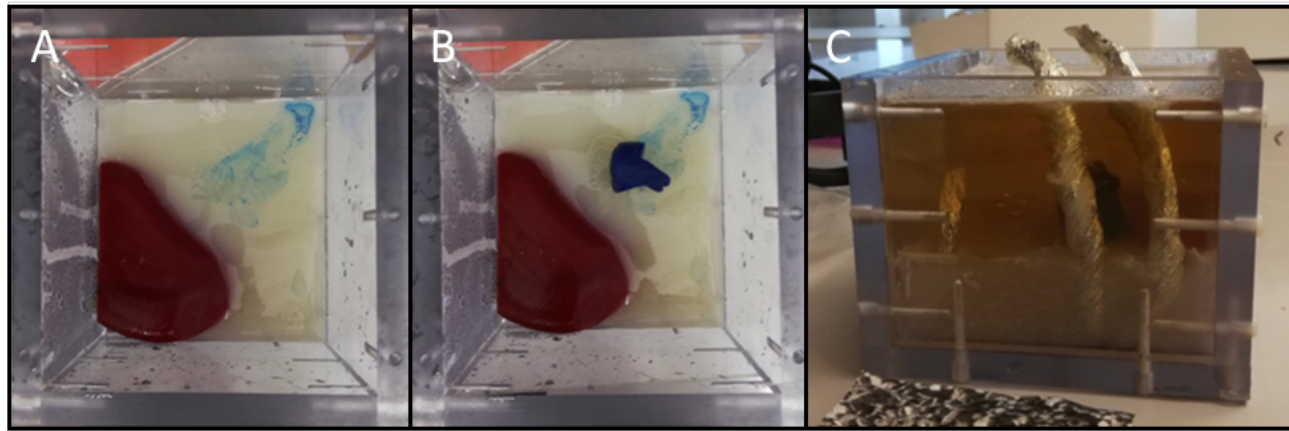


Figure 6. Model of phantom creation with **A:** Solely heart and surrounding tissue. **B:** Heart, lesion and surrounding tissue. **C:** Complete model with heart, lesion, and adjacent ribs, with the agar surrounding the lesion and ribs on the upper half of the phantom still unset, accounting for the temporary transparency.

3. RESULTS

Quantitative results after performing the biopsies on multiple phantoms are shown in Table I. An image of a tumor target and phantom is shown in Figure 7, as well as a cutaway image demonstrating the path of a needle in the phantom during a successful biopsy test. Biopsies performed using AR guidance produced lower mean distances to the center of the lesion. Additionally, the standard deviations were also smaller for AR guided biopsies, as has been seen previously^{14, 15}. We developed a phantom based on our patient CT data, complete with a synthetic tumor and bone. Our system was also successful in taking biopsies from this anatomically similar phantom (Figure 6).

Table I: Results from the phantom biopsy.

	Guidance Method	Mean Distance from Tumor Center (cm)	Mean Distance from Tumor Edge (cm)	Range (cm)
Soft Tissue Lesions	CT Image	1.52	0.44 ± 1.40	0.64
	AR	0.75	0.25 ± 0.88	0.44
Lung Lesions	CT Image	1.12	0.61 ± 0.40	0.92
	AR	0.62	0.35 ± 0.27	0.60

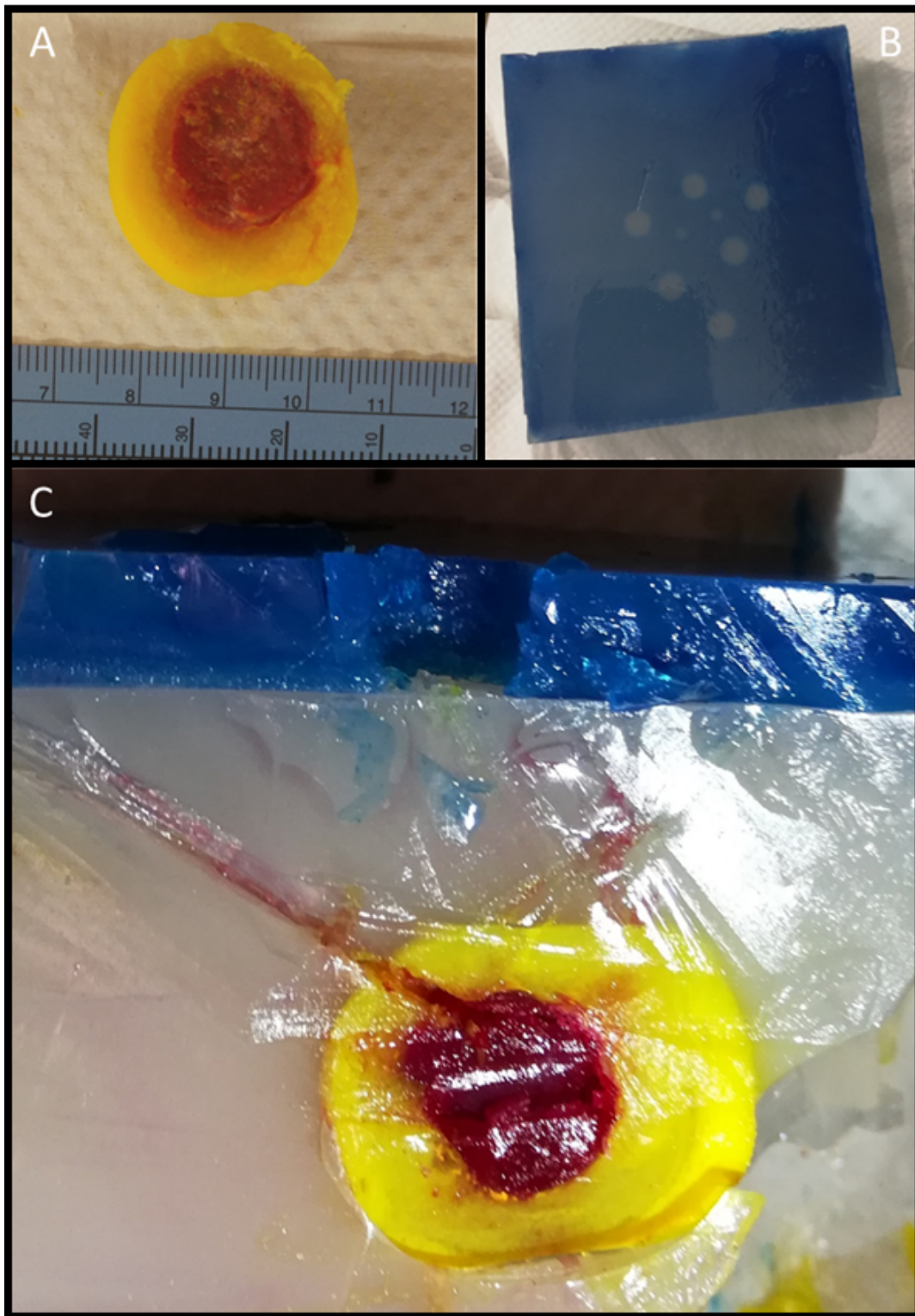


Figure 7. **A:** The tumor target (red) and neighboring tissue (yellow). **B:** A top view of the phantom with eight possible needle paths for the biopsy. The needle paths had two different sizes: six larger holes approximately 1 cm in diameter, and two narrow holes approximately 4 mm in diameter. **C:** A cutaway view of the tumor target in the phantom with a successful needle biopsy.

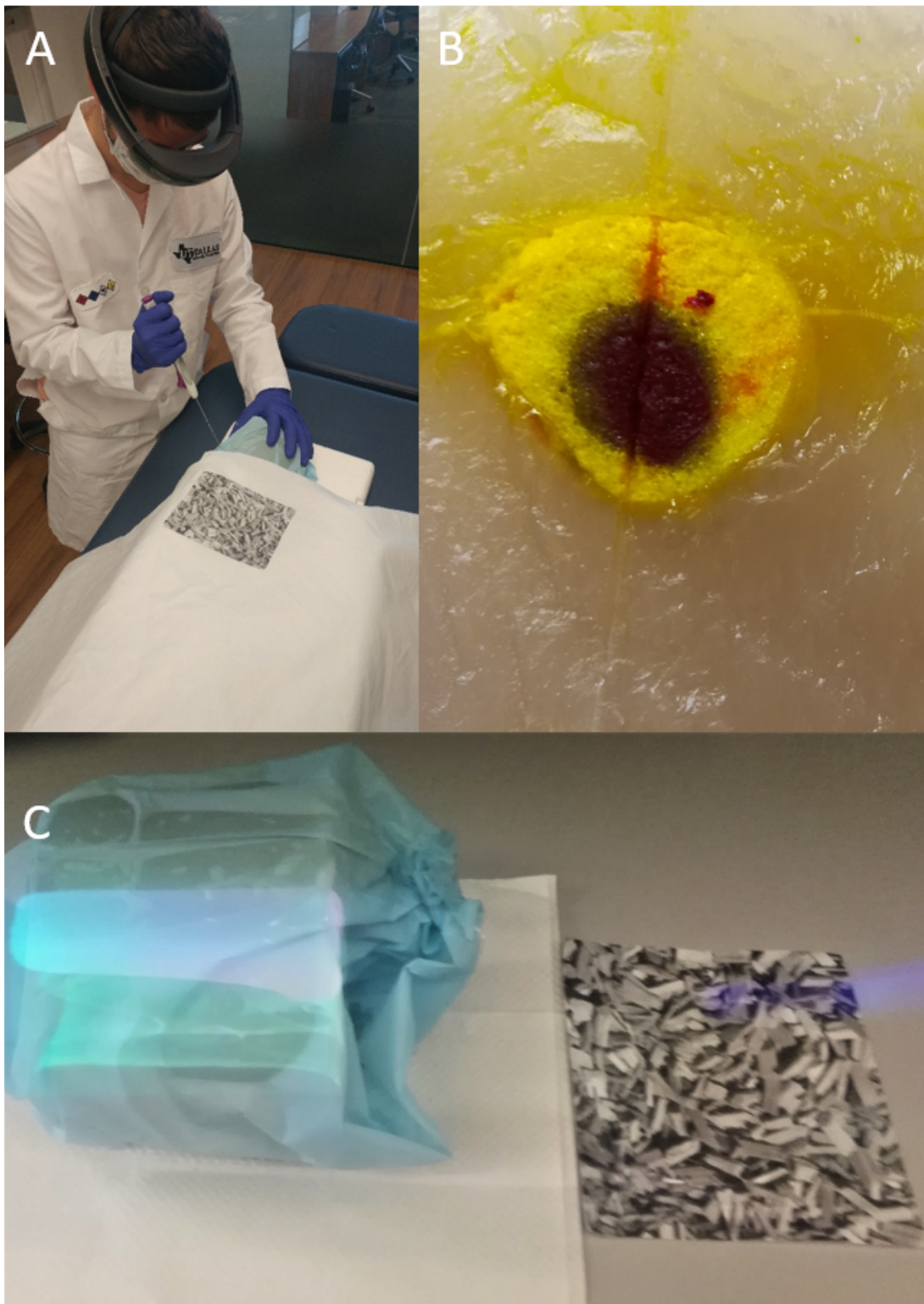


Figure 8: **A.** An example of how our system may be used in a clinical setting for a soft tissue lesion. **B.** A cross-sectional view of the biopsy needle path through the synthetic tumor (red) in the phantom. **C.** The view of the HoloLens model overlaid on the phantom.

4. DISCUSSION

Our system's strengths remain mainly in its adaptability and speed. We estimate that in a clinical setting, the entire post-CT imaging process of segmentation, model generation, hologram generation, and HoloLens deployment can be completed within 45 minutes to an hour as a conservative estimate, with manual segmentations requiring roughly 20-30 minutes of the total time. A time frame this short would make it extremely plausible to perform the biopsy directly following the patient's CT image maximizing accuracy by limiting the likelihood of significant organ shifting in the days following the CT imaging session.

One point of interest is that the AR guided biopsy acquisition requires slightly more time to obtain the cores due to the physician needing to constantly switch between looking at the hologram projected onto the glass versus the real-world biopsy needle. Generally, CT guided biopsy examples required roughly 3-10 minutes, depending on the number of cores that were extracted, as well as the complexity of the needle path. However, the increase of time is negligible, averaging to merely 2-4 more minutes per procedure. A greater potential issue rises upon prolonged HoloLens usage. After 15-30 minutes of prolonged HoloLens usage, the user will generally begin to experience a consistently increasing headache, where the only option is to remove the headset and allow one's eyes a 5-10 minute break to rest.

There were several limitations we encountered in this study. The first we encountered was that upon moving the models from 3D Slicer to Unity, the scale is not the same, requiring a change in the model scale in Unity. Moreover, the Vuforia image tracking software we employed to track the lower extremities requires a rather large image (10 cm by 7 cm) to guarantee consistent registration of the hologram to the real time patient which would be a major limitation in a clinical setting⁸. Yet the largest limitation currently experienced in this project remains that the HoloLens retains a highly limited field of view of 30 degrees in width by 17 degrees in height. Such a narrow field of view makes it very difficult to reliably view each portion of the procedure through the HoloLens as would be ideal, especially in a clinical setting in which a consistent and thorough understanding of every area is paramount to provide proper care⁸.

Additionally, we determined that much of our reported hologram drift is due to hardware limitations in the HoloLens' built-in hologram stability¹⁶. The HoloLens itself is not perfectly accurate in maintaining hologram position over time^{8, 14, 17}. As one rotates around the fiducial marker with the HoloLens, the system can shift the hologram away from the image position by an average of 4.15 mm laterally, 7.7 mm distally, and 6.05 mm vertically. Furthermore, the view of the HoloLens is limited to 1268 x 720 pixels per eye¹¹. This could reduce the flexibility of the HoloLens where high-resolution visualization is required, such as in the presence of small structures, and when a larger field-of-view is necessary.

5. CONCLUSION

In summation, we demonstrated the feasibility of using the HoloLens to visualize soft tissue biopsy targets as well as lung lesions, and how this visualization can be used to assist physicians in determining biopsy paths without additional real-time imaging. The system consistently outperformed biopsies performed solely by using CT images as guidance both in terms of accuracy and precision. However, the system does have a few limitations including a limited field of view, high hologram drift after large amounts of user motion, and the requirement of large fiducial markers.

Further work will incorporate automated model generation through the use of deep learning models and intensity thresholding to streamline the process and reduce the time required by a user to prepare the AR models for the biopsy. This has the potential to reduce the total time required per patient, thus increasing the number of patients seen per day. We will also explore the application of the presented method to additional clinical scenarios as well as other hardware systems, such as the HoloLens 2.

REFERENCES

- [1] Torriani, M., Etchebehere, M., and Amstalden, E. M. I., "Sonographically Guided Core Needle Biopsy of Bone and Soft Tissue Tumors," *Journal of Ultrasound in Medicine*, 21(3), 275-281 (2002).
- [2] Fei, B. W., Nieh, P., Master, V., Alemozaffar, M., Tade, F., Akin-Akintayo, O., Osunkoya, A., Goodman, M., and Schuster, D., "PET/Ultrasound fusion targeted biopsy of the prostate: initial clinical results," *Journal of Nuclear Medicine*, 58, 1 (2017).
- [3] Lee, S. M., Park, C. M., Lee, K. H., Bahn, Y. E., Kim, J. I., and Goo, J. M., "C-Arm Cone-Beam CT-guided Percutaneous Transthoracic Needle Biopsy of Lung Nodules: Clinical Experience in 1108 Patients," *Radiology*, 271(1), 291-300 (2014).
- [4] Xu, H., Lasso, A., Vikal, S., Guion, P., Krieger, A., Kaushal, A., Whitcomb, L. L., and Fichtinger, G., "MRI-Guided Robotic Prostate Biopsy: A Clinical Accuracy Validation," *Medical Image Computing and Computer-Assisted Intervention – MICCAI 2010*. 383-391.
- [5] Krücker, J., Xu, S., Glossop, N., Viswanathan, A., Borgert, J., Schulz, H., and Wood, B. J., "Electromagnetic Tracking for Thermal Ablation and Biopsy Guidance: Clinical Evaluation of Spatial Accuracy," *Journal of Vascular and Interventional Radiology*, 18(9), 1141-1150 (2007).
- [6] Dupuy, D. E., Rosenberg, A. E., Punyaratabandhu, T., Tan, M. H., and Mankin, H. J., "Accuracy of CT-Guided Needle Biopsy of Musculoskeletal Neoplasms," *American Journal of Roentgenology*, 171(3), 759-762 (1998).
- [7] Hau, M., Kim, J., Kattapuram, S., Hor nicek, F. J., Rosenberg, A. E., Gebhardt, M. C., and Mankin, H. J., "Accuracy of CT-guided biopsies in 359 patients with musculoskeletal lesions," *Skeletal Radiology*, 31(6), 349-353 (2002).
- [8] Huang, L., Collins, S., Kobayashi, L., Merck, D., and Sgouros, T., "Shared visualizations and guided procedure simulation in augmented reality with Microsoft HoloLens." 10951, 1095112.
- [9] Bernardino, M. E., Walther, M. M., Phillips, V. M., Graham, S. D., Sewell, C. W., Gedgaudas-McClees, K., Baumgartner, B. R., Torres, W. E., and Erwin, B. C., "CT-guided adrenal biopsy: accuracy, safety, and indications," *American Journal of Roentgenology*, 144(1), 67-69 (1985).
- [10] Manzey, D., Rottger S Fau - Bahner-Heyne, J. E., Bahner-Heyne Je Fau - Schulze-Kissing, D., Schulze-Kissing D Fau - Dietz, A., Dietz A Fau - Meixensberger, J., Meixensberger J Fau - Strauss, G., and Strauss, G., "Image-guided navigation: the surgeon's perspective on performance consequences and human factors issues," (1478-596X (Electronic)).
- [11] Hanna, M. G., Ahmed, I., Nine, J., Prajapati, S., and Pantanowitz, L., "Augmented Reality Technology Using Microsoft HoloLens in Anatomic Pathology," *Archives of Pathology & Laboratory Medicine*, 142(5), 638-644 (2018).
- [12] Frantz, T., Jansen, B., Duerinck, J., and Vandemeulebroucke, J., "Augmenting Microsoft's HoloLens with vuforia tracking for neuronavigation," *Healthcare Technology Letters*, 5(5), 221-225 (2018).
- [13] Mohandas, A., Ganesh, S., Jeevanandham, B., and Atkuri, P., "Augmented reality in medicine: technique, scope and status," *International Journal of Scientific Research*, VII, 57-58 (2018).
- [14] Li, M., Xu, S., Mazilu, D., Turkbey, B., and Wood, B. J., "Smartglasses/smartphone needle guidance AR system for transperineal prostate procedures." 10951, 109510Z.
- [15] Rosenthal, M., State, A., Lee, J., Hirota, G., Ackerman, J., Keller, K., Pisano, E. D., Jiroutek, M., Muller, K., and Fuchs, H., "Augmented reality guidance for needle biopsies: An initial randomized, controlled trial in phantoms†A preliminary version of this paper was presented at the Medical Image Computing and Computer-Assisted Intervention (MICCAI) 2001 conference in Utrecht. The Netherlands (Rosenthal et al., 2001)," *Medical Image Analysis*, 6(3), 313-320 (2002).
- [16] Vassallo, R., Rankin, A., Chen, E. C., and Peters, T. M., "Hologram stability evaluation for Microsoft HoloLens." 10136, 1013614.
- [17] Basafa, E., Foroughi, P., Hossbach, M., Bhanushali, J., and Stolka, P., "Visual tracking for multi-modality computer-assisted image guidance." 10135, 101352S.